# The Effect of Calcium Activation of Skinned Fiber Bundles on the Structure of *Limulus* Thick Filaments

Rhea J. C. Levine, John L. Woodhead, and Harriet A. King

Department of Anatomy and Neurobiology, The Medical College of Pennsylvania, Philadelphia, Pennsylvania 19129

*Abstract.* Here we present evidence that strongly suggests that the well-documented phenomenon of A-band shortening in *Limulus* telson muscle is activation dependent and reflects fragmentation of thick filaments at their ends.

Calcium activation of detergent-skinned fiber bundles of *Limulus* telson muscle results in large decreases in A-band (from 5.1 to 3.3 µm) and thick filament (from 4.1 to 3.3 µm) lengths and the release of filament end fragments. In activated fibers, maintained stretched beyond overlap of thick and thin filaments, these end fragments are translocated to varying depths within the I-bands. Here they are closely associated with fine filamentous structures that also span the gap between A- and I-bands and attach to the distal one-third of the thick filaments. End-fragments are rarely, if ever, present in similarly stretched and skinned, but unstimulated fibers, although fine "gap filaments" persist. Negatively stained thick filaments, separated from

skinned, calcium-activated, fiber bundles, allowed to shorten freely, are significantly shorter than those obtained from unstimulated fibers, but are identical to the latter with respect to both the surface helical array of myosin heads and diameters. Many end-fragments are present on grids containing thick filaments from activated fibers; few, if any, on those from unstimulated fibers. SDS-PAGE shows no evidence of proteolysis due to activation and demonstrates the presence of polypeptides with very high molecular weights in the preparations. We suggest that thick filament shortening is a direct result of activation in *Limulus* telson muscle and that it occurs largely by breakage within a defined distal region of each polar half of the filament. It is possible that at least some of the fine "gap filaments" are composed of a titin-like protein. They may move the activation-produced, fragmented ends of thick filaments to which they attach, into the I-bands by elastic recoil, in highly stretched fibers.

I**N** previous studies we determined that the decrease in A-band length during sarcomere shortening in *Limulus* telson muscles (de Villafranca, 1961; de Villafranca and Marschhaus, 1963; Levine et al., 1972) reflected, in part, an ~25% decrease in the length of constituent thick filaments (Dewey et al., 1973, 1977). We later found that short thick filaments (3.1 µm), separated from intact fibers that were stimulated to contract isotonically either electrically or by brief exposure to K⁺, had helical arrangements of surface subunits identical to those we described on the longer filaments (4.2 µm) separated from unstimulated fibers, and identical diameters (Levine et al., 1984; Levine and Kensler, 1985). This result implies that filament shortening reflects the loss of myosin and paramyosin from the thick filaments, rather than an internal rearrangement of the molecules.

K⁺ or electrical stimulation of intact fibers presumably causes release of Ca²⁺ from the sarcoplasmic reticulum. In *Limulus* muscle, which is dually regulated (Lehman et al., 1973), Ca²⁺ binds to troponin subunits on the thin filaments and, via a calmodulin-linked activation of endogenous myosin light chain kinase, causes phosphorylation of the regulatory light chains of myosin on the thick filaments (Sellers, 1981). To bridge the gap between sarcolemmal stimulation

and molecular events at the level of the thick filaments, we have examined the effects of both direct Ca²⁺ activation of detergent-skinned fiber bundles of *Limulus* telson muscle and in vitro phosphorylation of myosin regulatory light chains of native thick filaments separated from unstimulated fibers, on thick filament structure and, where applicable, A-band length. In this paper we report the results of Ca²⁺ activation of skinned fiber bundles on these parameters.

## Materials and Methods

### Tissue Preparation

Bundles of *Limulus* telson levator muscles were dissected free from the animal, with their origins on the opisthosomal carapace and insertions into posterior tendons intact. Some bundles were tied at their origins and insertions and stretched to nonoverlap in a lucite chamber, while immersed in relaxing solution (0.1 M KCl, 5 mM MgCl₂, 2 mM EGTA, 2 mM ATP, 1 mM DTT, 0.4 mM NaAz, 7 mM phosphate buffer, pH 6.8) at 4°C. This tissue was used for light and electron microscopic examination of longitudinal sections. Other bundles were carefully separated from their origins, frayed with a forceps and immersed in relaxing solution at 4°C. These bundles were used for separation of thick filaments. The solution bathing both types of bundles was changed three times over a four to six hour period. All muscle bundles were then immersed in relaxing solution containing

0.5% Triton-X 100 and gently stirred or shaken for 1 h at 4°C. Detergent was removed from the muscle by washing with three changes of relaxing solution without detergent. Experimental bundles were then $Ca^{2+}$-activated by 40-s to 1-min immersion in activating solution (relaxing solution, either without EGTA and with 1 mM $CaCl_2$ and protease inhibitors [Sellers, 1981] added, or containing 2 mM EGTA with 4 mM $CaCl_2$ added), by which time the stretched bundles produced tension (seen by breakage of a few fibers as they attempted to shorten) and the free bundles shortened by ∼50%. Control bundles were not exposed to activating solution.

## Microscopy

After activation, stretched bundles were rinsed briefly with relaxing solution. Both these and the control stretched bundles were fixed for light and electron microscopy by dropwise delivery of 0.3% glutaraldehyde in mincing solution (0.1 M KCl, 5 mM $MgCl_2$, 2 mM EGTA, 1 mM DTT, 7 mM phosphate buffer, pH 6.8) until they stiffened, followed by immersion in 3% glutaraldehyde in the same buffer for from 3 h to overnight. These bundles were cut transversely into pieces ∼5 mm long, which were postfixed in 1% aqueous $OsO_4$, rinsed, dehydrated in a graded acetone series and propylene oxide, and embedded in Epon. One micrometer thick longitudinal sections, containing ∼5 mm lengths of the muscle bundles, were cut with freshly made glass knives. Silver sections were cut with a Diatome diamond knife on a Sorvall-Reichert ultramicrotome (Sorvall Instruments Div., Newton, CT) from blocks trimmed to 1.5 mm in their longest dimension. The knife edge was always parallel to the long axis of the fiber bundle. The one micrometer sections were stained with toluidine blue, mounted under coverslips on glass slides and viewed and photographed at a final magnification of 1,600 using a Leitz Orthoplan light microscope, a yellow filter over the condenser, and Kodak Pan-X 35 mm film. The silver sections were mounted on formvar-coated or naked 400-mesh copper grids, stained with 1% uranyl acetate and lead citrate and viewed and photographed at nominal magnifications of 3,500, 5,800, 9,800, 19,000, 27,000, and 36,000 on Kodak EM film using a JEOL 100CX electron microscope with a 30-μm objective aperture in place, at an accelerating voltage of 80 kV. Magnifications were calibrated using a calibration grid with 2,156 lines/in.

## Filament Preparation and Microscopy

After activation, freely shortened fiber bundles were rinsed with relaxing solution and both these and the control "free" bundles were kept in fresh relaxing solution for from 4 h to overnight. They were then gently homogenized in fresh relaxing solution and thick filaments were separated, adsorbed onto medium thickness carbon films on 300-mesh copper grids and negatively stained with 1% uranyl acetate as previously described (Kensler and Levine, 1982; Levine and Kensler, 1985). Electron microscope images were obtained at a nominal magnification of 19,000 on Kodak EM film, in the JEOL 100CX electron microscope at an accelerating voltage of 80 kV, with an anticontamination device in operation. Magnifications were calibrated as described above.

## Measurements

Sarcomere, A-band, I-Z-I-band, and gap-region lengths were measured on prints of known magnification made from the light micrographs of sectioned fiber bundles, since the 1-μm sections contained greater lengths of the fibers than the thin sections did. These measurements were checked by measuring single sarcomeres from the same fibers on the negatives of electron micrographs taken at magnifications of 3,600 and 5,800. Mean lengths and standard deviations were obtained for each of the above parameters in experimental and control bundles and compared using $t$ test. Two such comparisons were made: in one, no attempt was made to separate the two fiber types in the muscle: one having large diameters, long sarcomeres, A-bands and thick filaments and one having small diameters, extremely long sarcomeres, A-bands and thick filaments (Levine et al., 1989). In the second, the same parameters were compared between experimental and control bundles, within each fiber type.

Filament lengths were measured directly on electron microscope negatives of the negatively stained, separated filaments. Only intact filaments having a central bare zone and two tapered ends were included in the population of measured filaments. The lengths of filament fragments were also measured. Mean filament lengths and standard deviations were obtained for experimental and control populations of isolated thick filaments and compared. In this analysis, we did not separate filament populations that were released from the two fiber types.

## Image Analysis

Electron micrograph negatives of negatively-stained control and experimental isolated filaments were scanned on an Optronics P1000 rotary-drum scanning densitometer interfaced with a VAX 1180 minicomputer and diffraction patterns computed from the scans were displayed on an AED 757 graphics terminal and photographed on 35-mm Kodak Pan-X film. Layerlines out to the sixth or seventh were selected by computerized masking of the diffraction pattern to produce filtered images, which were displayed on the graphics terminal and photographed.

## SDS-PAGE

Samples of control and experimental muscle bundles that were allowed to shorten freely were prepared for SDS-PAGE by homogenization and boiling for 3 min in sample buffer. These were run in pairs (experimental, control) at loadings of 5, 10, and 15 μg on 7.5% and 5% minigels. The gels were fixed, stained with Coomassie brilliant blue, and destained in methanol. The 7.5% gels were examined for the presence of differences in the banding pattern between the experimental and control samples and the 5% gels were used to detect the presence of very high molecular weight bands. The gels were photographed using Polaroid 55P/N film.

# Results

## Sectioned Fiber Bundles

**Light Microscopy.** Each longitudinally sectioned bundle contains between seven and twenty fibers. Both large-diameter, long sarcomere and small-diameter, very long sarcomere fibers are present (Levine et al., 1989). In light micrographs of toluidine blue-stained, 1-μm sections of stretched fiber bundles, an unstained gap separates the A- and I-bands in both control and experimental (activated) bundles, indicating that the sarcomeres were stretched beyond overlap of thick and thin filaments (Fig. 1). There is no difference in mean sarcomere length: 13.2 vs. 13.2 μm between all experimental and all control fibers (Table I). The small differences in mean sarcomere lengths between experimental and control fibers of the same type: 12.7 (control) vs. 12.3 μm (experimental) for large-diameter fibers; 13.8 (control) vs. 14.5 μm (experimental) for small-diameter fibers, are neither consistent with their history of activation, nor significant (Table I). These results indicate that minimal if any sarcomere shortening occurred due to activation.

The appearance of the sarcomeres in activated fibers is, however, markedly different from that of the controls. In the latter, the A-bands are long and, especially in large-diameter fibers, have relatively even edges. Frequently, the central A-band is bisected by a light-staining line, or pseudo-H-zone, indicative of thick filament alignment. In these control fibers, the ends of the thin filaments, on either side of the Z-lines (comprising the I-Z-I-band measured) are also in register, producing evenly marked I-bands, which are well separated from the A-band edges by fairly narrow, unstained gap regions (Fig. 1 a). In all control fibers, the mean lengths of the A-, I-Z-I-bands and gap regions are, respectively: 5.1, 5.5, and 1.2 μm (this last measurement is per half-sarcomere in this and all succeeding cases). In large-diameter fibers, the mean lengths for these parameters are: 4.8, 5.0, and 1.2 μm. For small-diameter fibers they are: 5.5, 6.0, and 1.2 μm.

Activated fibers of both types have shorter A-bands, with more ragged edges, than the controls. Invariably, the I-Z-I-bands in stretched fibers of all activated bundles are shorter, less regular and stain much more intensely, even more in-
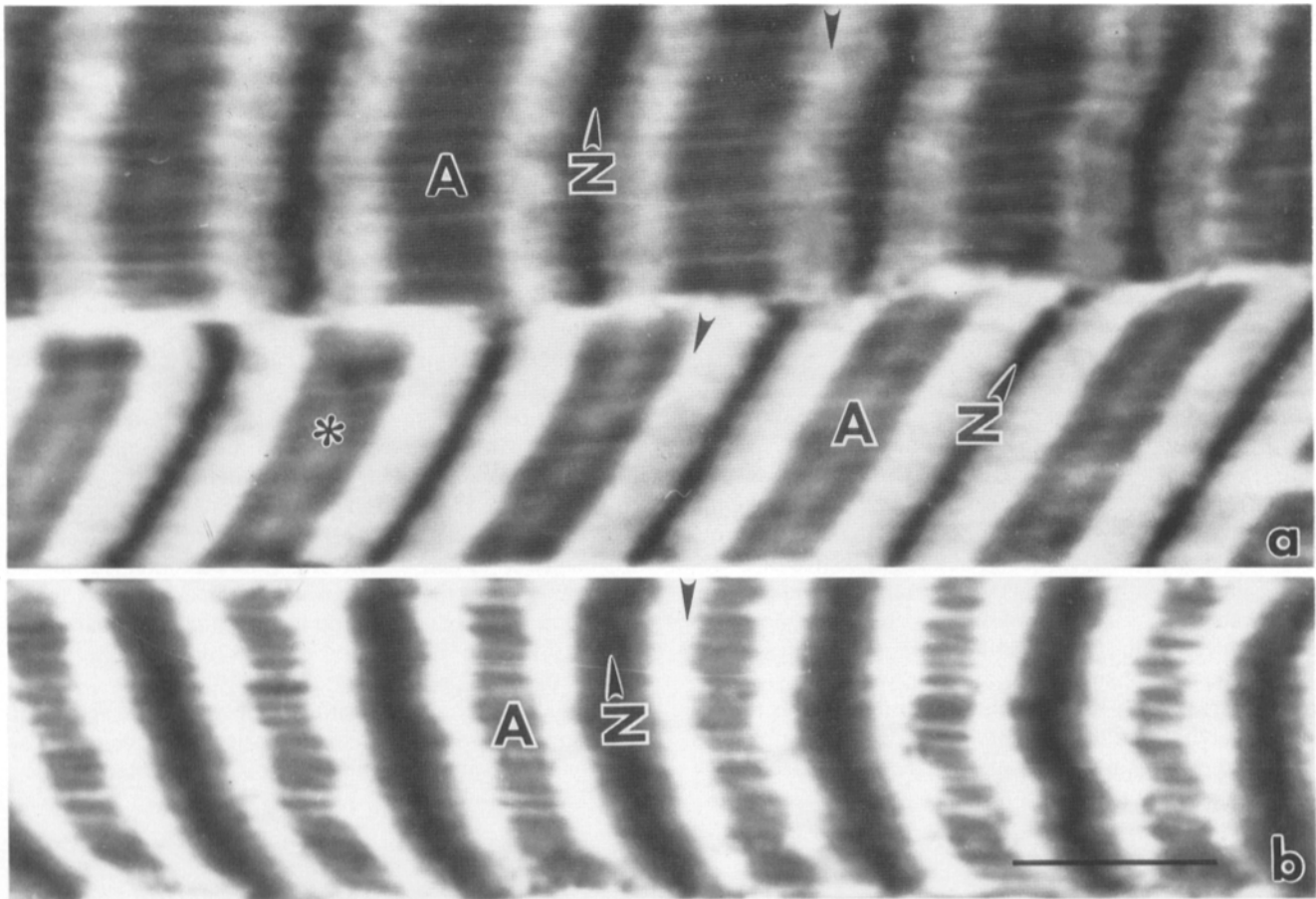
*Figure 1.* Light micrographs of toluidine blue–stained, semithin (1 μm) sections of detergent-skinned *Limulus* telson fiber bundles, stretched beyond overlap of thick and thin filaments. A-bands and Z-lines are labeled. (*a*) Two fibers in a control bundle. The upper fiber is of the small diameter type, the lower of the large diameter type. Note the longer sarcomeres and A-bands in the upper fiber. The A-band edges are more ragged than in the lower fiber. In the lower fiber the pseudo-H-zone, marked by the asterisk, in the center of the A-bands is clearly visible. Light-staining "gap-regions" indicated by the arrowheads, are seen between the A- and I-bands in both fibers. (*b*) One fiber (large diameter type) in an experimental bundle. Note decreases in the lengths of both the A- and I-bands and the increased staining of the I-Z-I band in these fibers. The apparent width of the "gap-regions" (*arrowheads*) is also larger than in the control fibers. Bar, 10 μm.

tensely than the A-bands, than in the controls. The gap-region between the A- and I-bands is increased in the activated fibers (Fig. 1 *b*). Overall mean lengths of A-, I-Z-I-bands and gap regions of activated fibers are, respectively: 3.3, 4.3, and 2.9 μm (Table I). For large-diameter fibers these parameters measure: 2.7, 4.2, and 2.8 μm; for small-diameter fibers:

4.0, 4.5, and 3.0 μm. In both fiber types the experimentally induced differences (decreases in A- and I-Z-I-band and increase in gap-region lengths) are significant to $p \leqslant 0.0005$ (Table I).

Occasionally, broken fibers, with greatly shortened sarcomeres, are seen in the experimental bundles. From such im-

*Table I. Mean Lengths of Sarcomeres and Regions*

| | Sarcomere | A-band* | I-Z-I* | Gap (half-sarcomere)* |
|---|---|---|---|---|
| | | μm ± SD | | |
| Control fibers | | | | |
| All ( n = 167) | 13.2 ± 1.27 | 5.1 ± 0.42 | 5.5 ± 0.70 | 1.2 ± 0.14 |
| Small diameter (n = 71) | 13.8 ± 0.30 | 5.5 ± 0.00 | 6.0 ± 0.22 | 1.2 ± 0.16 |
| Large diameter (n = 96) | 12.7 ± 1.21 | 4.8 ± 0.23 | 5.2 ± 0.69 | 1.2 ± 0.11 |
| Activated fibers | | | | |
| All (n = 85) | 13.2 ± 1.10 | 3.3 ± 0.71 | 4.3 ± 0.31 | 2.9 ± 0.33 |
| Small diameter (n = 38) | 14.5 ± 0.48 | 4.0 ± 0.26 | 4.5 ± 0.39 | 3.0 ± 0.13 |
| Large diameter (n = 47) | 12.3 ± 0.71 | 2.7 ± 0.24 | 4.2 ± 0.13 | 2.8 ± 0.21 |

* Differences in lengths of A-bands, I-Z-I bands, and gap regions between experimental and control fibers are statistically significant to $p \leqslant 0.005$.

ages it appears that on release from stretch, thin and thick filaments can reinterdigitate to shorten activated fibers. The most highly shortened fibers are buckled and have sarcomere lengths of <3.0 μm. It is impossible to obtain any other measurements from these. No I-bands are visible in these sarcomeres and the Z-lines appear thickened. A few shortened fibers appear to have been prevented from actual breakage, possibly by retaining membraneous connections to the tendon. Such fibers have sarcomere lengths between 3.5 and 4.0 μm and retain discernible, but very narrow, I-bands and normal-looking Z-lines and also have short A-bands (≤3.0 μm).

## EM

Measurements of selected sarcomeres from the same fibers analyzed by light microscopy were made on electron micrograph negatives of longitudinally sectioned bundles, and these agree with the light microscopic results. No attempt was made to measure thick filament lengths directly from sectioned fiber bundles, since even a slight degree of obliquity of the section might affect this parameter. The electron micrographs were used primarily to determine fine structural changes in the organization of the sarcomeres of the highly stretched fiber bundles after activation.

The decrease in A-band length of activated fibers is readily apparent and, as indicated above, agrees with measurements from light microscopy. The ragged edges of the A-bands of activated fibers only, are seen to consist of bent and wavy extensions of thick filaments (Compare Figs. 2 and 3). Many of these structures appear to be separated from the rest of the filament, but this may be due to some degree of section obliquity. This appearance is similar to that of relaxed, highly stretched frog muscle (cf. Fig. 3, Higuchi et al., 1988), but in our hands occurs only in activated fibers.

The spaces between A- and I-bands in electron micrographs of both control and experimental fiber bundles, stretched beyond overlap, are occupied by a meshwork of fine filaments that, even at low magnification, appears to overlap slightly with the ends of thick filaments in the A-bands. Activated fibers additionally show the presence of longitudinally-oriented, dark-staining structures, from ~0.2 up to 1.0 μm long, that penetrate the I-bands to different extents and are enmeshed within a network of thin filaments and the fine, filamentous material (Fig. 3). At higher magnifications, (>5,800) these dark-staining structures are identifiable as fragments of thick filaments (Fig. 3 b). The presence of such fragments is limited to activated fibers maintained beyond overlap; in fibers that had broken and thus shortened during activation, the I-bands are too narrow and the A-bands too dense to permit visualization of thick filament fragments, even if they are present.

Also at higher magnification, fine filaments appear to form a more-or-less longitudinally oriented mesh in the gap regions of sarcomeres of both control and activated bundles.
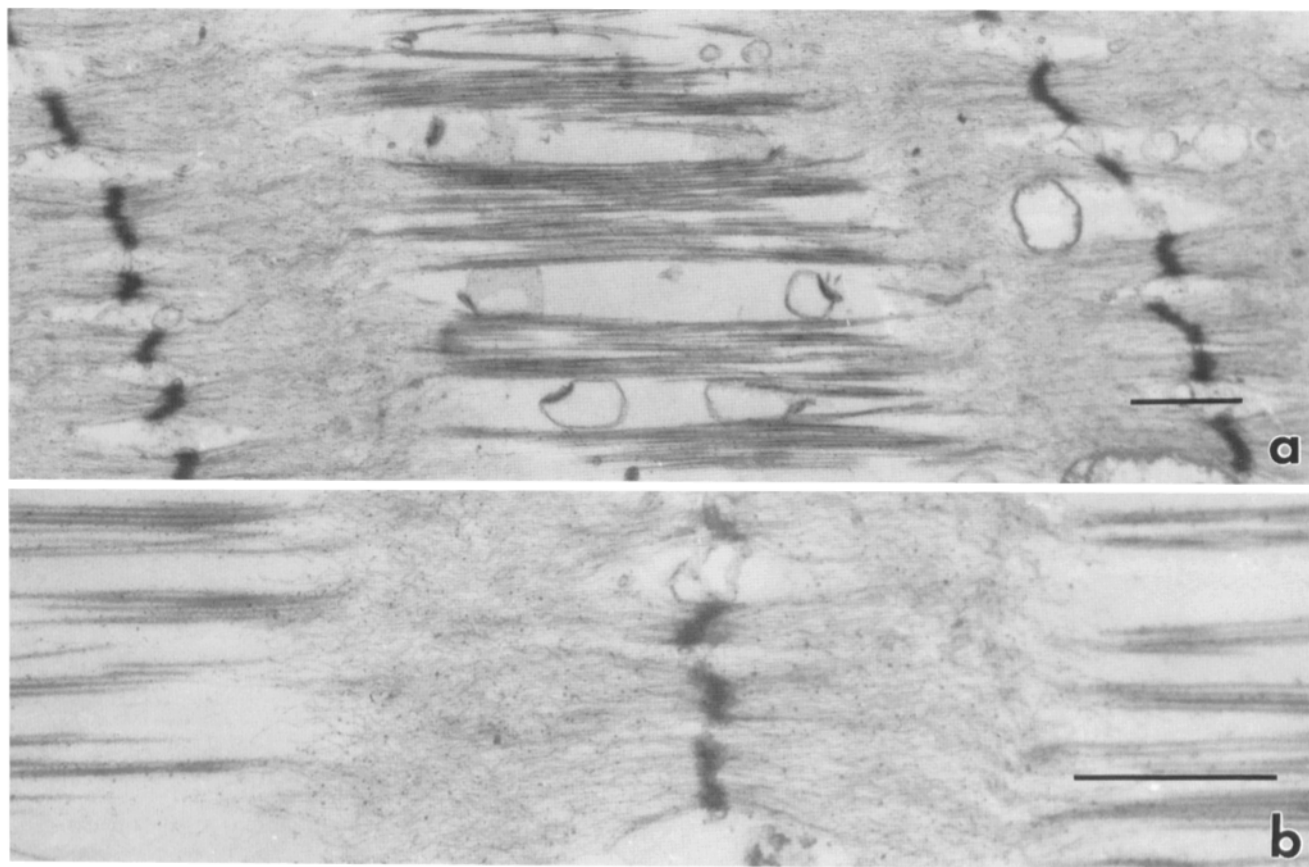


*Figure 2.* Electron micrographs of a sarcomere in a skinned, control bundle. (*a*) Low magnification micrograph, showing a complete sarcomere. (*b*) Medium magnification micrograph centered on the I-Z-I region of a sarcomere in the same fiber as above. Only thin filaments and very fine filamentous material is seen in the I-bands. Bars, 1 μm.
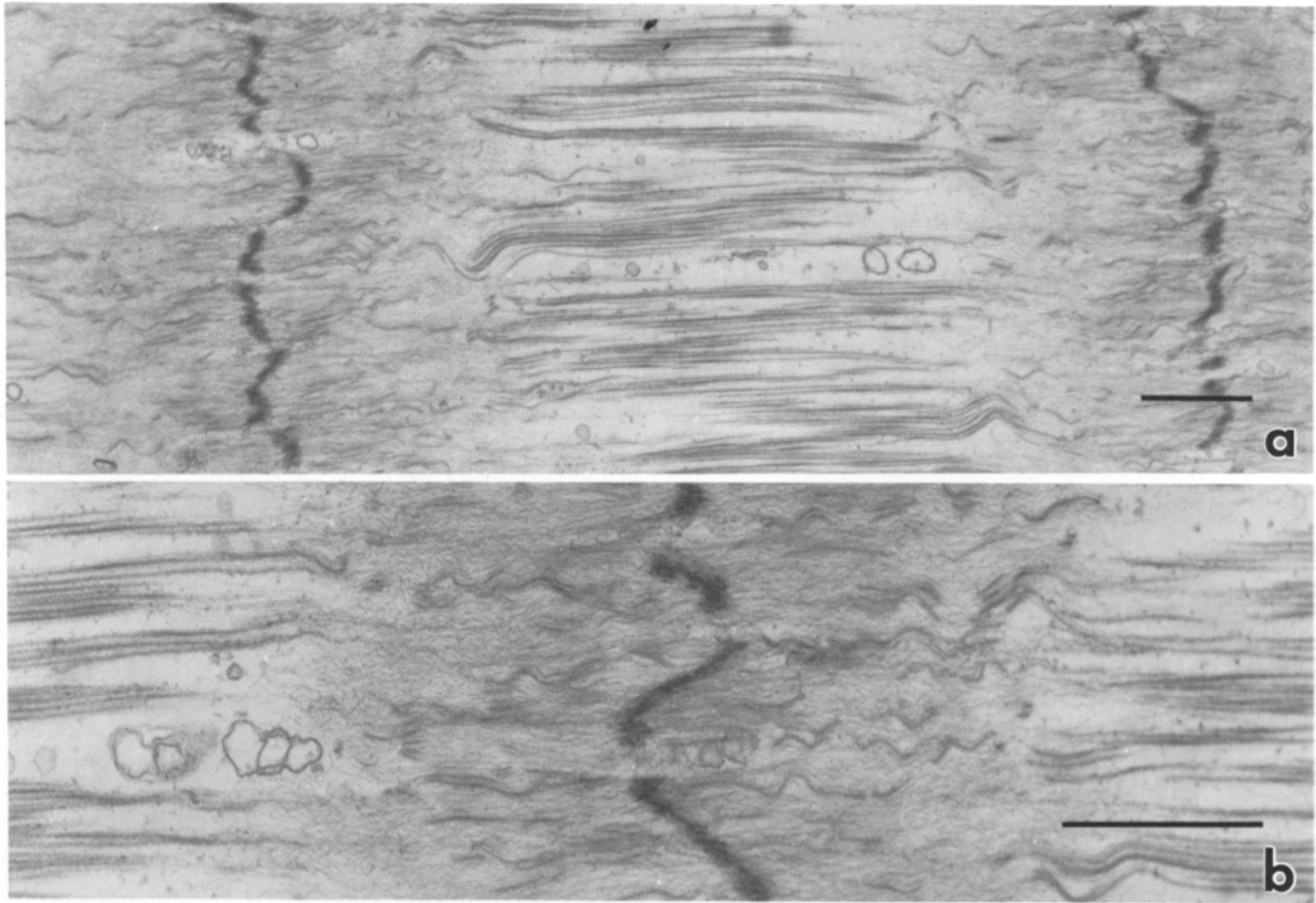
*Figure 3.* Electron micrographs of a sarcomere in a skinned, $Ca^{2+}$-activated bundle. (*a*) Low magnification micrograph, showing the complete sarcomere. Note the wavy ends (some disconnected) of thick filaments in the A-bands, and increased electron density of the I-bands. (*b*) Medium magnification micrograph centered on the I-Z-I region of a sarcomere in the same fiber as shown in the micrograph above. Note the presence of numerous end-fragments of thick filaments throughout the I-bands. These fragments have assumed a wavy configuration. Bars, 1 $\mu$m.

It is not clear whether these "gap filaments" are disarrayed ends of thin filaments or different structures. Some of them connect with lateral regions of the thick filaments, but do not extend deep into the A-band (Fig. 4 *a*). In experimental fibers the gap filaments are somewhat less longitudinally disposed than in the controls: the meshwork appears more open and breaks are seen (Fig. 4 *b*). Connections still exist between the gap filaments and the ends of thick filaments in the A-bands. More striking, however, is the presence of nearly periodic connections between the gap filaments and the thick filament fragments in the I-bands. Each thick filament fragment appears to be "caged" by surrounding fine filaments and held in place by quasi-periodic struts extending from them (*arrowheads* in Fig. 4 *b*). Indeed, the I-bands of experimental fibers are so occupied by thin filaments, thick filament fragments and fine filamentous meshes that individual structures are difficult to distinguish. It is probable that this increased protein content, in the smaller volume of the I-bands of activated fibers, is responsible for the intense I-Z-I-band staining in light micrographs.

## Separated Thick Filaments

On inspection of electron micrographs of negatively-stained preparations, most of the thick filaments separated from both $Ca^{2+}$-activated and control fiber bundles show good helical order. No difference is discernible in either filament diameter or the arrangement of surface subunits between the two populations (compare Figs. 5 and 6) although there is a highly significant difference in mean filament length ($p \leqslant 0.005$). 218 filaments measured on electron microscope negatives of control grids have a mean length of 4.11 $\pm$ SD 0.36 $\mu$m. The shortest intact filaments from unstimulated fiber bundles are 3.5 $\mu$m and the longest, 6.1 $\mu$m (Fig. 7). 16% of this population includes thick filaments of 4.5 $\mu$m or longer. Presumably, these are separated from the small diameter fibers having very long sarcomeres and A-bands and comprising ~18% of the cross-sectional area (Levine et al., 1989). A few fragments are present on control grids: the majority of these are derived from thick filaments that had broken at the bare zone region, probably during homogenization of the fiber bundles. 598 filaments measured on electron microscope negatives of experimental grids have a mean length of 3.25 $\pm$ SD 0.66 $\mu$m. The differences in mean filament length between the control and activated populations is highly significant ($p \leqslant 0.005$). The shortest intact filaments from $Ca^{2+}$-activated fiber bundles are 2.25 $\mu$m and the long-
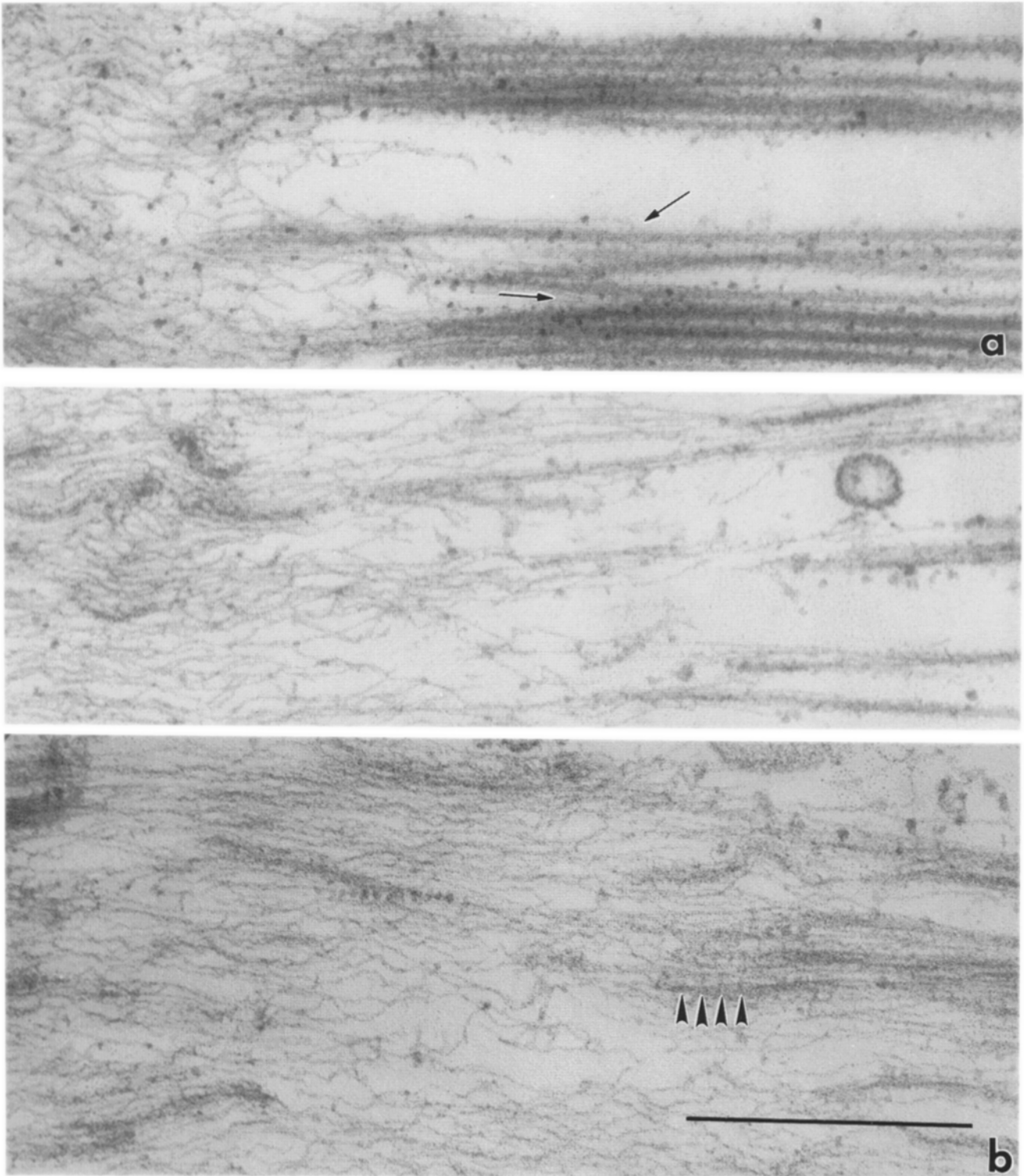
*Figure 4.* Electron micrographs of the gap-regions of sarcomeres from skinned fiber bundles, stretched beyond overlap. (*a*) Higher magnification micrograph of the gap region in a sarcomere from a control bundle. Note the filamentous meshwork. Single connections between fine "gap filaments" and distal regions of some thick filaments are indicated by small arrows. No connections are seen more centrally in the A-bands. No end-fragments of thick filaments are visible. (*b*) Higher magnification micrographs of the gap regions in two different sarcomeres from Ca$^{2+}$-activated bundles. Note the continued presence of the filamentous meshwork, as well as end-fragments of thick filaments. In the lower micrograph, end-fragments and distal regions of thick filaments appear to be "caged" by a nearly periodic arrangement of cross-struts (*arrowheads*), extending between gap filaments. Bar, 0.5 μm.
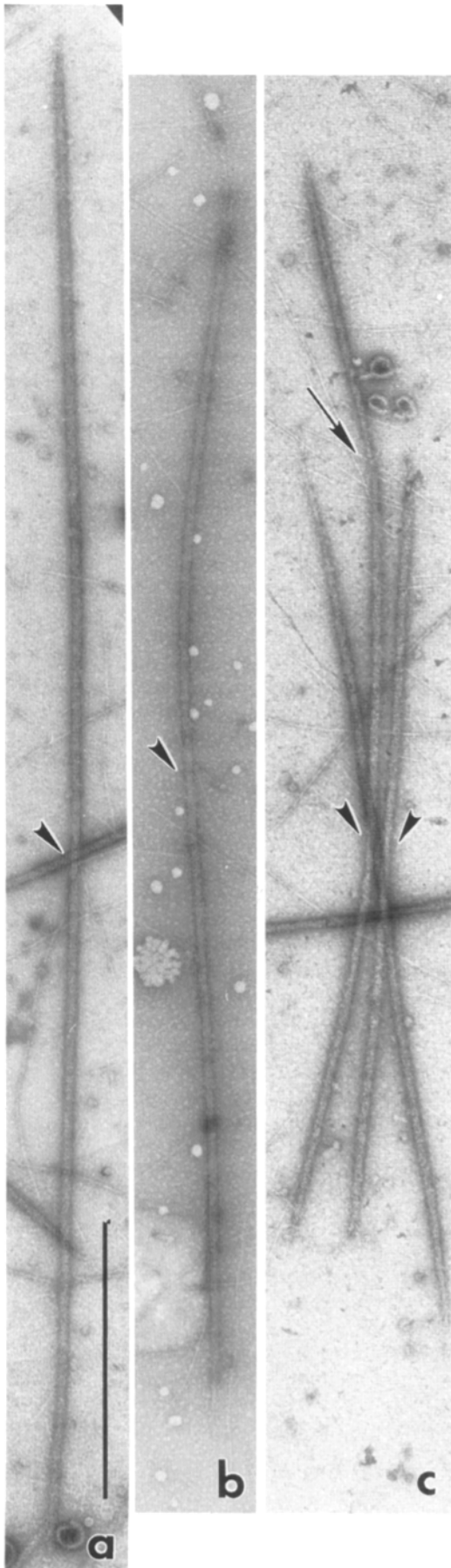
est, 5.6 $\mu$m. 16% of this population are 3.75 $\mu$m or longer (Fig. 7). The longest (4.5 $\mu$m and over) constitute ∽5% of the entire experimental filament population and may have been released from some of the very long sarcomere fibers that had not been effectively activated. Many of these longer filaments show distinct uni- or bilateral distal bends. The bent portion was included in the measurement if the overall length of that polar half-filament was the same as that of the intact half with opposite polarity. Many fragments, frequently closely associated with one or both ends of a thick filament, are seen on grids made from experimental bundles (Fig. 5 c). The fragments have the same helical structure as the isolated filaments. Measurements made of 143 fragments reveal that they belong to either one of two length populations: one with a mean length of 0.63 $\mu$m and one with a mean length of 1.17 $\mu$m. The fragments always have at least one tapered end, similar to those at the ends of intact filaments. Occasionally, both ends of the fragments are tapered, but in most instances the end opposite the tapered one abruptly narrows to a smooth, cylindrical projection, devoid of myosin periodicity (Fig. 6 b) and reminiscent of the appearance of the paramyosin cores obtained from myosin-stripped *Limulus* thick filaments (Levine et al., 1982, 1988).

## Image Analysis

Virtually identical diffraction patterns were computed for helical periodicity on the surfaces of filaments separated from both control and experimental bundles, and the filtered images obtained from the layer-line information on the diffraction patterns show the same structural features and repeats in both cases (Fig. 8).

## Gel Electrophoresis

There is no difference in the banding pattern between the control and experimental fiber bundles on the 7.5% gels (Fig. 9 a). This indicates that it is highly unlikely that any proteolysis occurred during activation. A distinct band of very high molecular weight is seen to have entered the separating portion of the 5% gels, and three faint bands between it and the myosin heavy chain band are also visible (Fig. 9 b). It is possible that the very high molecular weight band represents titin, or a titin-like protein, while the three faint bands may indicate the presence of nebulin-like polypeptides.

*Figure 5.* A gallery of electron micrographs of negatively-stained thick filaments, separated from skinned *Limulus* telson fiber bundles (*arrowheads* indicate bare zones). (*a* and *b*) Thick filaments separated from skinned, control fiber bundles. (*a*) Example of a "very long" thick filament that probably derives from the small diameter fibers. (*b*) Example of a "long" thick filament, similar to most of those obtained from relaxed fibers in previous work. (*c*) An example of a group of thick filaments obtained from a skinned fiber bundle that was Ca²⁺-activated and allowed to shorten freely. Note the decreased length of the filaments, and the presence of an end fragment in association with one end of one short filament (*arrow*). There is no apparent difference in surface structure among the filaments shown in *a*, *b*, or *c*. Bar, 1 $\mu$m.
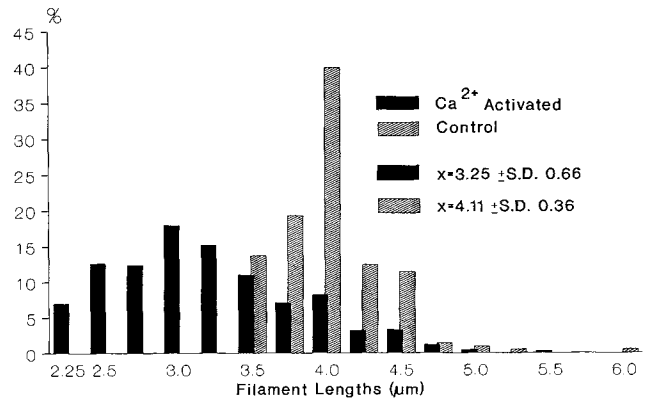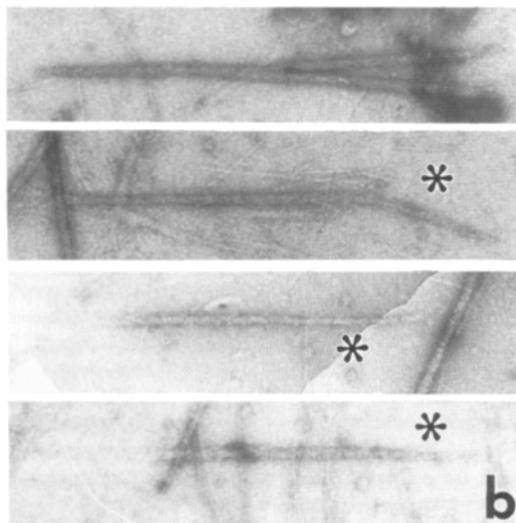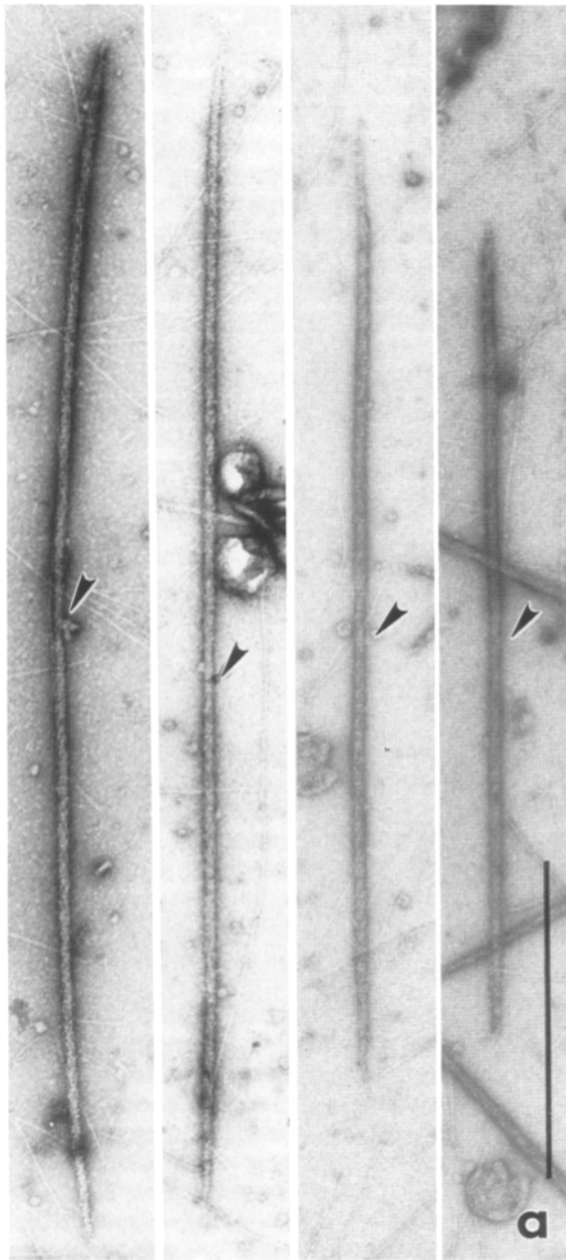
Figure 7. Histogram of the distribution of thick filament lengths measured on electron micrograph negatives of negatively-stained preparations of control and experimental fiber bundles. Only complete thick filaments with central bare zones were included in these measurements. No intact filaments <2.25 μm were seen on grids made from activated preparations and no intact filaments <3.5 μm were seen on those from controls.

## Discussion

Both light micrographs of toluidine blue–stained, 1 μm thick, longitudinal sections and electron micrographs of thin sections of stretched, skinned, $Ca^{2+}$-activated fibers reveal that A-band shortening, previously reported in isotonically contracting fibers and myofibrils of *Limulus* striated muscle, is a thick filament response to activation that is independent of sarcomere length. The gap between the A- and I-bands in micrographs of both control and activated fiber bundles indicates that the fibers were stretched to sarcomere lengths beyond which the thick and thin filaments overlap and that this sarcomere length was maintained during activation. The increase in length of the gap region in the sarcomeres of activated fibers further underscores the effect of activation on the length of A-bands and thick filaments. Thus, the situation in *Limulus* fibers is unlike that reported for frog skeletal muscle, where active sarcomere shortening, either loaded (Periasamy et al., 1990) or unloaded, to delta state contraction (Huxley, H. 1990. *Biophys. J.* 57:543a.) is required for A-band shortening.

The increased density of the I-Z-I region in light micrographs of activated fibers probably reflects, in part, the electron microscopic finding of thick filament fragments within the I-bands of these fibers. Both of these observations corre-

Figure 6. Electron micrographs of negatively-stained thick filaments obtained from skinned, $Ca^{2+}$-activated *Limulus* telson fiber bundles. (a) A gallery of negatively-stained thick filaments from activated fiber bundles. bare zones are indicated by arrowheads. These filaments have identical surface structure and diameters to those in Fig. 5 a, b, and c. (b) End fragments of thick filaments found almost exclusively on grids of experimental preparations. Note the decreased diameter at one end of most of the fragments (*asterisks*). The two size classes usually found are represented by the two upper micrographs (longer fragments) and the two lower ones (shorter fragments). Bar, 1 μm.
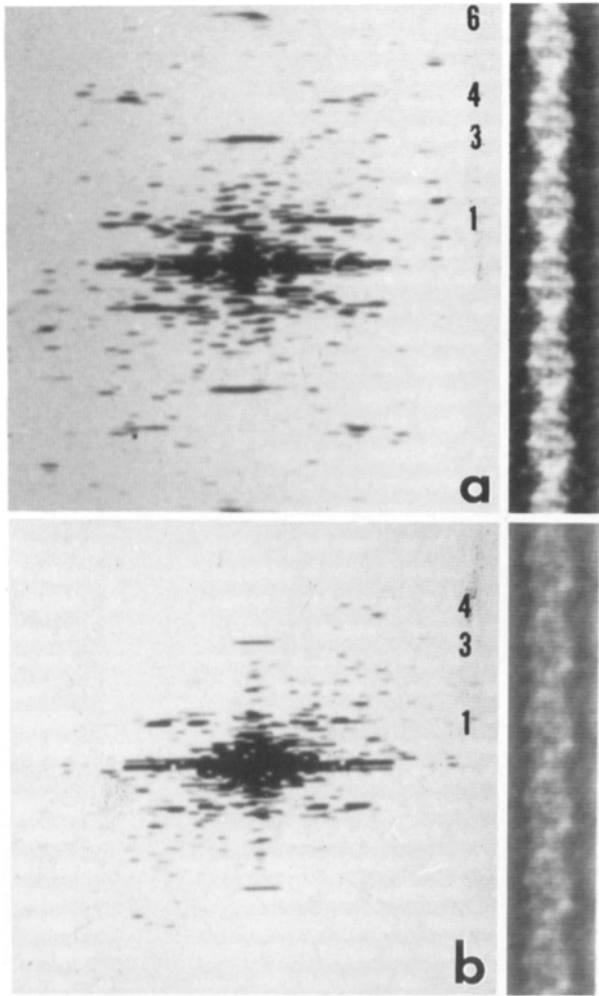
*Figure 8.* Computer-derived Fourier transforms and filtered images obtained from negatively-stained thick filaments separated from skinned *Limulus* telson fiber bundles. Layer lines on the transforms are numbered. (*a*) Transform and filtered image obtained from an image of a 4.2-$\mu$m-long thick filament separated from a skinned, relaxed (*control*) fiber bundle. (*b*) Transform and filtered image obtained from an image of a 3.2-$\mu$m-long thick filament released from a skinned, $Ca^{2+}$-activated fiber bundle. Filtered images were obtained by masking off all layer lines that were present on the computed transform (in fact, up to seven were present in the control transform, and the first, third, fourth and 6th layer lines were used from the experimental one). There is essentially no difference in the surface periodicity between the control and experimental filaments, although the staining of the control preparation was better than that of the experimental one.

late with the appearance of bends, breaks, and fragments of filament ends, together with short thick filaments, in negatively stained preparations from skinned, $Ca^{2+}$-activated fiber bundles, allowed to shorten freely. It is unlikely that homogenization during filament separation was solely responsible for breakage near the ends of thick filaments, since preparations from skinned, control fiber bundles contain few fragments and most of these are half-filaments, broken in the bare zone. Therefore, filament end fragmentation and short A-bands and thick filaments are associated with
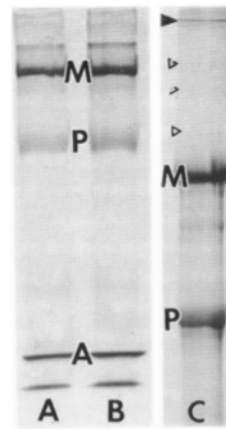


*Figure 9.* SDS-polyacrylamide slab gels, loaded with *Limulus* myofibrillar protein. (*a*) 7.5% gel. Lane *A* was loaded with 10 $\mu$g of protein from a control fiber bundles. Lane *B* was loaded with 10 $\mu$g of protein from a $Ca^{2+}$-activated fiber bundle. *M* = myosin heavy chain bands, *P* = paramyosin bands, *A* = indicates actin bands. There is no apparent difference in the banding patterns between the control and experimental lanes, indicating that no proteolysis occurred due to the activation. (*b*) 5% gel, loaded with 15 $\mu$g of *Limulus* myofibrillar protein from a relaxed, skinned fiber bundle. Dark triangle indicates very high molecular weight polypeptide (possibly titin, or a similar protein) that has just entered the separating gel. Light triangles indicate three high molecular weight bands, between the putative titin band and the myosin heavy chain band. *M* = myosin heavy chain bands, *P* = paramyosin bands, *A* = actin bands.

$Ca^{2+}$-activation of *Limulus* fibers, whether they are maintained at sarcomere lengths beyond overlap, or allowed to shorten freely.

The possibility that the fragmentation of thick filaments observed in all experimental preparations is due to $Ca^{2+}$ activation of endogenous protease activity must be considered. It is doubtful that such degradation of thick filament protein occurs, however, since all experimental preparations include either EGTA or a protease inhibitor cocktail. SDS-PAGE of experimental and control-separated filament preparations show no differences between them. The absence of bands with increased mobility on gels of experimental preparations indicates that proteolysis is unlikely to account for filament end-fragmentation. Additionally, re-examination of micrographs of filament preparations made from intact fiber bundles stimulated to contract isotonically by exposure to high $K^+$ (Levine and Kensler, 1985), reveals the presence of thick filament fragments of the same lengths as those described here. No $Ca^{2+}$ was added to, and EGTA was always present in, the solutions used in the earlier experiments.

There is a considerable range in the lengths of thick filaments separated both from control and experimental fiber bundles, although the means of the two populations are significantly different. In part, this length range is due to the presence of at least two fiber types in each muscle bundle. We have already shown that most thick filaments will be separated from large-diameter fibers, which have average filament lengths of ~4.1 $\mu$m and the remainder from small-diameter, very long sarcomere fibers with thick filaments that can be >6 $\mu$m long (Levine et al., 1989). However, there is still a considerable range of filament lengths present. It may be that, as we observed with histochemical staining for myofibrillar ATPase and mitochondrial $\beta$-NADH diaphorase activities, there are as many as four different types of fibers present in *Limulus* telson muscles. Each of these may have filaments that differ somewhat in length, and may contain different isoforms of myosin and/or paramyosin. Alternatively, aside from the real differences between the two fiber

types described above, the mechanism of length regulation for *Limulus* thick filaments may be less precise than it is for those of vertebrate striated muscle. In any case, the difference in mean filament length between experimental and control preparations is not only significant, but disappears if the lengths of the fragments seen in the experimental preparations are added to each end of the shorter filaments. Although there is overlap in filament lengths between experimental and control preparations at the longer end of the scale, intact filaments (having central bare zones) <3.5 μm in length are never seen on control grids. The very long filaments are rarely found in experimental preparations. When present, they are usually bent at one or both ends (the length of the bends is the same as that of the longer class of fragments) and would be >2 μm shorter if the bent end or ends were not included in the measurement.

The presence of bent filament ends, the same length as the free filament end-fragments present in both sections and filament preparations of experimental bundles, suggests that the latter result directly from fiber activation and not secondarily by the reassociation of disaggregated myosin and paramyosin molecules. In fact, in vitro attempts to coprecipitate *Limulus* myosin and paramyosin to produce synthetic filaments with native periodicity have been largely unsuccessful. The individual proteins precipitate independently: myosin forms short, mainly aperiodic, albeit bipolar, structures and paramyosin forms paracrystals. Obviously, the two proteins precipitate to form thick filaments in vivo. However, there is no information available on striated muscle development or myofibrillar protein turnover in *Limulus* that might provide either a model for, or a means of, establishing the parameters governing thick filament or fragment assembly. A "breakage" hypothesis for shortening of *Limulus* thick filaments is further supported by the identical periodicity of the helical arrangement of myosin heads on the surfaces of fragments and both long and shortened filaments.

From a functional viewpoint, it is important to determine the fate of the broken ends of filaments during muscle contraction. In these studies, when sarcomeres are maintained in a highly stretched state, filament fragments are translocated into the I-bands, despite the absence of overlap between thick and thin filaments before, during, and after activation. Titin, a massive protein (Maruyama et al., 1984; Trinick et al., 1984) that extends from near the M-line to connect individual thick filaments to the Z-line in vertebrate striated muscle (Maruyama et al., 1985; Pierobon-Bormioli et al., 1989), and may be responsible for regulation of thick filament length (Whiting et al., 1989), has not been definitely identified in or extracted from *Limulus* muscle. Other arthropod muscle contain a minititin, however, and antibodies raised against this protein crossreact with *Limulus* muscle (Nave and Weber, 1990). Nevertheless, the presence of very high molecular weight polypeptides on 5% gels, suggest that a more massive form of titin, or a similar protein, as well as one identical, or similar, to nebulin (another sarcoskeletal protein of vertebrate-striated muscle [Maruyama et al., 1989; Pierobon-Bormioli et al., 1989; Wang, 1984; Wang and Wright, 1988]) may occur in *Limulus* striated muscle. It may be that a titin-like protein constitutes at least some of the fine filamentous structures that occupy the gap between the A- and I-bands in the highly stretched sarcomeres. If so, then

unlike the situation in vertebrate muscle (Whiting et al., 1989), these structures do not extend beyond the lateral one-third of *Limulus* thick filaments, into the sarcomere centers. Thus, it is possible that release of filament end fragments by activation events under abnormally large passive tensions, as produced in these experiments, may produce a recoil effect in some of these elastic molecules, moving them, together with associated thick filament fragments, into the I-band. A secondary effect of such elastic recoil is the bunching and bending of the thin filaments, resulting in the decrease in the length of the I-Z-I band that we observe. Horowits and Podolsky (1987) demonstrated that radiation damage to titin in one half-sarcomere of rabbit fibers causes the translocation of entire A-bands to the other end of the sarcomere, during contraction. Also, Higuchi et al. (1988) showed, but did not comment on, shortened A-bands with misaligned thick filaments and the presence of thick filament fragments in the I-bands of frog semitendinosus fibers stretched to sarcomere lengths of 5 μm. These observations may be related to our finding of thick filament end-fragments in the I-bands of highly-stretched, Ca$^{2+}$-activated, skinned *Limulus* fibers. We plan to determine whether or not the high molecular weight band on our gels is similar to vertebrate titin, and to attempt to localize this protein in *Limulus* sarcomeres, first using mono- and polyclonal antibodies to the vertebrate polypeptide and/or, if necessary, raising monoclonals to the band excised from gels of *Limulus* muscle.

Thick filament end fragmentation similar to that observed in highly stretched fibers probably also occurs in the shortened, activated fibers, since the latter have short A-bands and thick filaments. Moreover, the A-band density is increased and the interfilament spacing appears smaller in the shortened sarcomeres than in those that remained stretched beyond overlap. Thus, the filament end fragments may be retained within the overlap region where they may contribute to the increased A-band density. Indeed, thick filament ends may even completely bend over within the A-bands, while remaining partially attached to the rest of the filament. Since the time to develop peak tension is relatively slow (up to 1 min) in electrically stimulated *Limulus* telson fibers, and relaxation can be even slower (up to 10 min.) in this muscle (Davidheiser and Davies, 1982; Walcott and Dewey, 1980), there is probably sufficient time for filament ends to either bend over and restraighten or dissociate and reanneal during a contractile event. We plan to examine the sarcomere length tension relations in single fibers, since such unusual internal changes in the structure of the contractile apparatus should be reflected by measurable mechanical states.

If breakage of the distal regions of the filaments is the main mechanism of thick filament shortening in *Limulus* muscle, it is likely that the myosin, and perhaps also the paramyosin, molecules in the breakage zone are biochemically different from those in the rest of the thick filament. These specifically located molecules may respond uniquely to the events after Ca$^{2+}$ activation. Distinct myosin isoforms (A and B) have been localized to different regions of the paramyosin-containing thick filaments of the body wall muscles of the nematode, *C. elegans* (Epstein et al., 1985, 1986; Miller et al., 1983), although the functional significance of this topographic distribution is not known. A similar situation may exist in *Limulus*, with the function of enabling thick fila-

ments to fit into sarcomeres shortened to their minimum in situ length ($\leqslant$4.0 $\mu$m: Levine et al., 1972; Dewey et al., 1973, 1977).

Since *Limulus* muscle is dually regulated (Lehman et al., 1973), one event initiated by $Ca^{2+}$ activation is the calmodulin-dependent phosphorylation of myosin regulatory light chains (Sellers, 1981). In the companion paper (Levine et al., 1991) we will describe the effect of in vitro light chain phosphorylation on the structure of thick filaments separated from relaxed *Limulus* telson levators.

## References

Davidheiser, S., and R. E. Davies. 1982. Energy utilization of *Limulus* telson muscle at different sarcomere lengths. *Am. J. Physiol.* 242:R394–R400.

de Villafranca, G. W. 1961. The A- and I-band lengths in stretched or contracted horseshoe crab skeletal muscle. *J. Ultrastruct. Res.* 5:109–115.

de Villafranca, G. W., and C. M. Marschhaus. 1963. Contraction of the A band. *J. Ultrastruct. Res.* 9:156–165.

Dewey, M. M., R. J. C. Levine, and D. E. Colflesh. 1973. Structure of *Limulus* striated muscle. The contractile apparatus at different sarcomere lengths. *J. Cell Biol.* 58:573–593.

Dewey, M. M., B. Walcott, D. E. Colflesh, H. Terry and R. J. C. Levine. 1977. Changes in thick filament length in *Limulus* striated muscle. *J. Cell Biol.* 75:366–380.

Epstein, H. F., D. M. Miller III, I. Ortiz, and G. C. Berliner. 1985. Myosin and paramyosin are organized about a newly identified core structure. *J. Cell Biol.* 100:904–915.

Epstein, H. F., I. Ortiz, and L. A. Traeger Mackinnon. 1986. The alteration of myosin isoform compartmentation in specific mutants of *Caenorhabditis elegans. J. Cell Biol.* 103:985–993.

Higuchi, H., T. Yoshioka, and K. Maruyama. 1988. Positioning of actin filaments and tension generation in skinned muscle fibres released after stretch beyond overlap of the actin and myosin filaments. *J. Muscle Res. Cell Motil.* 9:491–498.

Horowits, R., and R. Podolsky. 1987. The positional stability of thick filaments in activated skeletal muscle depends on sarcomere length: evidence for the role of titin filaments. *J. Cell Biol.* 105:2217–2223.

Kensler, R. W., and R. J. C. Levine. 1982. An electron microscopic and optical diffraction analysis of the structure of *Limulus* telson muscle thick filaments. *J. Cell Biol.* 92:443–451.

Lehman, W., J. Kendrick-Jones, and A. G. Szent-Gyorgyi. 1973. Myosin-linked regulatory systems: comparative studies. *Cold Spring Harbor Symp.*

*Quant. Biol.* 37:319–330.

Levine, R. J. C., and R. W. Kensler. 1985. Structure of short thick filaments from *Limulus* muscle. *J. Mol. Biol.* 182:347–352.

Levine, R. J. C., M. M. Dewey, and G. W. de Villafranca. 1972. Immunohistochemical localization of contractile proteins in *Limulus* striated muscle. *J. Cell Biol.* 55:221–236.

Levine, R. J. C., R. W. Kensler, M. Stewart, and J. C. Haselgrove. 1982. Molecular organization of *Limulus* thick filaments. *In* Basic Biology of Muscles: A Comparative Approach, editors. B. M. Twarog, R. J. C. Levine, and M. M. Dewey. Raven Press, New York. 37–52.

Levine, R. J. C., R. W. Kensler, M. C. Reedy, W. Hofmann, S. Davidheiser, and R. E. Davies. 1984. Structure of *Limulus* and other invertebrate thick filaments. *In* Contractile Mechanisms in Muscle. G. H. Pollack and H. Sugi, editors. Plenum Publishing Corp., New York. pp. 93–106

Levine, R. J. C., P. D. Chantler, and R. W. Kensler. 1988. Arrangement of myosin heads on *Limulus* thick filaments. *J. Cell Biol.* 107:1739–1748.

Levine, R. J. C., S. Davidheiser, R. W. Kensler, A. M. Kelly, J. Leferovich, and R. E. Davies. 1989. Fiber types in *Limulus* telson muscles: morphology and histochemistry. *J. Muscle Res. Cell Motil.* 10:53–66.

Maruyama, K., H. Sawada, S. Kimura, K. Ohashi, H. Higuchi, and Y. Umazume. 1984. Connectin filaments in stretched fibers of frog skeletal muscle. *J. Cell Biol.* 99:1391–1397.

Maruyama, K., T. Yoshioka, H. Higughi, K. Ohashi, S. Kimura, and R. Natori. 1985. Connectin filaments link thick filaments and Z lines in frog skeletal muscle as revealed by immunoelectron microscopy. *J. Cell Biol.* 101:2167–2172.

Maruyama, K., A. Matsuno, H. Higuchi, S. Shimaoka, S. Kimura, and T. Shimizu. 1989. Behaviour of connectin (titin) and nebulin in skinned muscle fibres released after extreme stretch as revealed by immunoelectron microscopy. *J. Muscle Res. Cell Motil.* 10:350–359.

Miller, D. M. III, I. Ortiz, G. C. Berliner, and H. F. Epstein. 1983. Differential localization of two myosins within nematode thick filaments. *Cell.* 34:477–490.

Nave, R., and K. Weber. 1990. A myofibrillar protein of insect muscle related to vertebrate titin connects Z band and A band: purification and molecular characterization of invertebrate mini-titin. *J. Cell Sci.* 95:535–544.

Periasamy, A., D. Burns, D. Holdren, G. Pollack, and K. Trombitas. 1990. A-band shortening in single fibers of frog skeletal muscle. *Biophys. J.* 57: 815–829.

Pierobon-Bormioli, S., R. Betto, and G. Salvati. 1989. The organization of titin (connectin) and nebulin in the sarcomeres: an immunocytolocalization study. *J. Muscle Res. Cell Motil.* 10:446–456.

Sellers, J. 1981. Phosphorylation-dependent regulation of *Limulus* myosin. *J. Biol. Chem.* 256:9274–9278.

Trinick, J., P. Knight, and A. Whiting. 1984. Purification and properties of native titin. *J. Mol. Biol.* 180:331–356.

Walcott, B., and M. M. Dewey. 1980. Length-tension relation in *Limulus* striated muscle. *J. Cell Biol.* 87:204–208.

Wang, K. 1984. Cytoskeletal matrix in striated muscle: the role of titin, nebulin and intermediate filaments. *In* Contractile Mechanisms in Muscle. G. H. Pollack and H. Sugi, editors. Plenum Publishing Corp., New York. 285–306.

Wang, K., and J. Wright. 1988. Architecture of the sarcomere matrix of skeletal muscle: immunoelectron microscopic evidence that suggests a set of parallel inextensible nebulin filaments anchored at the Z line. *J. Cell Biol.* 107:2199–2122.

Whiting, A., J. Wardale, and J. Trinick. 1989. Does titin regulate the length of muscle thick filaments? *J. Mol. Biol.* 205:263–268.